DST: Differential Spatiotemporal Learning for Contactless Electrocardiogram Reconstruction

Yuping Wang
Beijing University of Posts and Telecommunications
Beijing, China
wyuping@bupt.edu.cn

Shuai Zhao *
Beijing University of Posts and Telecommunications
Beijing, China
zhaoshuaiby@bupt.edu.cn

Qizheng Wang
Beijing University of Posts and Telecommunications
Beijing, China
buptwqz@bupt.edu.cn

Jianquan Zhang
Beijing University of Posts and Telecommunications
Beijing, China
zjq0701@bupt.edu.cn

Junliang Chen
Beijing University of Posts and Telecommunications
Beijing, China
chjl@bupt.edu.cn

***Abstract*—Continuous cardiac monitoring has been a challenge in contactless vital sign detection using mmWave radar systems. However, existing approaches primarily focus on the heartbeat detection and often fail to achieve comprehensive electrocardiogram (ECG) reconstruction. Therefore, a synergistic approach is proposed that integrates signal differential algorithm and spatiotemporal learning model (DST) to enable high-precision, contactless ECG monitoring. Initially, a differential method is used to achieve cardiac acceleration signal from the radar signals. Subsequently, a cascaded spatiotemporal learning model is proposed to extract spatial and temporal features of the cardiac acceleration signal. Experimental results indicate that our DST approach achieves timing precision with 90-percentile mean absolute error of 5.0 ms and morphological accuracy with 90-percentile Pearson-Correlation of 0.981 and Root-Mean-Square-Error of 0.17 compared to the ground-truth ECG.**

***Index Terms*—mmWave radar, contactless ECG monitoring, spatiotemporal learning, waveform reconstruction**

I. Introduction

Continuous cardiac monitoring serves as a critical component in contemporary vital sign monitoring, offering substantial clinical benefits by enabling timely intervention for high-risk individuals and early detection of life-threatening conditions, including cardiac arrhythmias [1], acute myocardial infarction [2], sudden infant death syndrome [3], and cerebrovascular events [4]. However, contact-based ECG detection is unsuitable for long-term monitoring and is not applicable to daily assessments. Therefore, contactless-based monitoring has become a promising approach. Compared with other sensors such as cameras and acoustic sensors with privacy issues, radar could achieve strong robustness under light conditions or temperature variations [5], [6].

The earliest attempt at radar-based respiration monitoring was achieved by measuring the chest wall displacement induced by respiration in 1975 [7]. Thereafter, various advanced algorithms have been developed to exploit different intrinsic characteristics for reconstructing coarse cardiac information (e.g. heart rate [8], heart cycle [9]). For example, the Kalman filter uses the predicted value and uncertainty to further update and optimize the band-pass filter (BPF) to achieve heart rate tracking [10]. Although this method improves the accuracy of heart rate estimates, it cannot extract fine-grained cardiac events. In addition, Nguyen et al. [11] used ensemble Empirical Mode decomposition (EEMD) to reduce mode aliasing, but the introduced noise affected the accuracy of the results. Z. L.Xia et al. [12] applied variational mode decomposition (VMD) to the separation of respiratory and heartbeat in the vital signs, which improves the accuracy of the separated instantaneous frequencies of respiratory and heartbeat components. However, one disadvantage of VMD is that it requires setting the number of decomposition layers and penalty factors, which can lead to problems such as under-decomposition or over-decomposition. In recent years, the emergence of commercial radar platforms with high operating frequency (mmWave radar) encourages researchers to extract fine-grained cardiac features, such as seismocardiography (SCG) and ECG. For instance, U. Ha et al. [13] used 1D-CNN to construct a mapping relationship from RF signal to SCG signal to realize the reconstruction of SCG waveform, and the correlation coefficient between the predicted signal and the actual signal was above 0.72. D. Toda et al. [14] proposed a method that body surface displacement signal obtained from Frequency-Modulated Continuous Wave (FMCW) radar is used as input of CNN to reconstruct ECG signal. The results showed that the mean absolute error (MAE) of R peaks were 102.2 ms and the median correlation coefficient between the predicted and the actual signal is 0.86. However, the displacement signal contains breathing and other noises, which are not conducive to obtaining high reconstruction accuracy. J. Chen et al. [15] proposed an end-to-end network to convert radio frequency

* Corresponding author: Shuai Zhao. This work was supported by National Natural Science Foundation of China (Grant No.6247204 U21A20468).

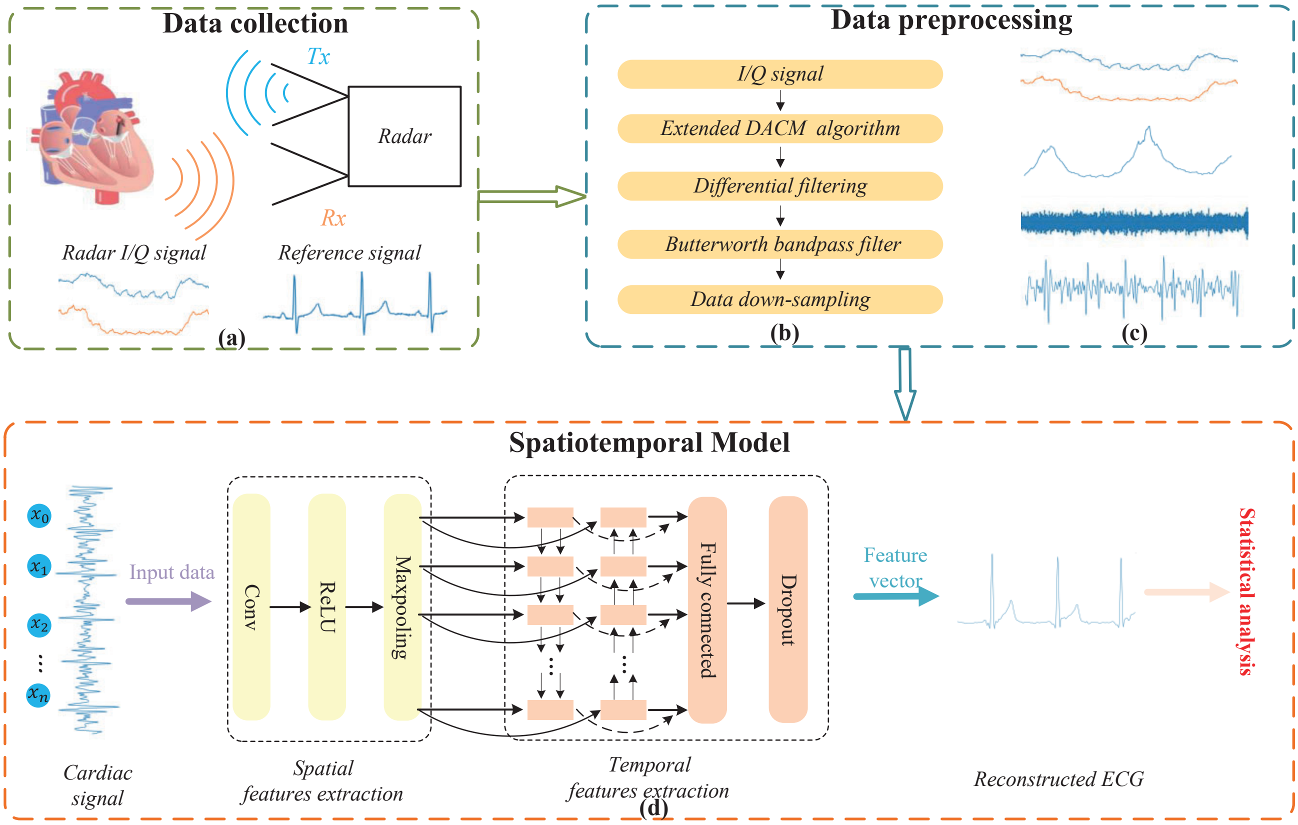

Fig. 1. System overview

(RF) signal into ECG signal, with a median correlation coefficient of 0.90. The most existing studies merely employ deep learning methods to extract the conversion information from enormous coarse-grained radar signal to ECG signal relying on the non-linear mapping ability of the deep neural network. Although these studies could successfully reconstruct the ECG signal from radar, some drawbacks still need to be improved:

First, coarse-grained radar data contains plenty of noises such as respiration and body movement, weakening the subtle features and affecting the performance of neural network.

Second, pure data-driven deep learning approaches rarely utilize prior knowledge of the data during training process, such as mathematical/physical models of the problem itself, resulting in the inability to verify.

To deal with above limitations, a method that integrates signal differential methods and cascaded spatiotemporal learning model is proposed to achieve high-quality cardiac signal and improve the performance. It is not a mere combination but a theory-guided data-driven paradigm, preserving the interpretability of signal methods while empowering systems to handle complex time series signal efficiently. The main contributions are as follows:

Initially, we proposed a signal-processing-driven cascaded spatiotemporal learning framework, which is a cross-modal mapping mechanism from non-contact radar micro-motion signals to electrocardiogram signals.

Then, the signal preprocessing module at the front end of the cascaded network can suppress noise component that are detrimental to the neural network's performance, retain the subtle cardiac features that are critical for accurate construction, and provide a verifiable physically meaningful initial feature space for subsequent model.

Finally, comprehensive experiments demonstrate that the proposed method can exhibit outstanding performance in both morphological accuracy and timing precision.

II. MODEL

System overview of the proposed method is described as Fig. 1, which mainly includes data collection, radar signal preprocessing and ECG reconstruction model. The following section will primarily focus on the latter two.

A. Radar Signal Preprocessing

First, the signal from radar needs to be preprocessed to obtain the chest displacement of mixed heartbeat and breathing components.

Assuming that the initial distance between the radar and the human chest is , and the change in surface micro-displacement caused by physiological activities is $x(t)$. By down-converting the received signal, the in-phase $(I(t))$ and quadrature $(Q(t))$ baseband signals can be obtained, which are expressed as:

$$I(t) = A\cos\left(\theta_0 + \frac{4\pi x(t)}{\lambda} + \Delta\phi\right) \tag{1}$$

$$Q(t) = A\sin\left(\theta_0 + \frac{4\pi x(t)}{\lambda} + \Delta\phi\right) \tag{2}$$

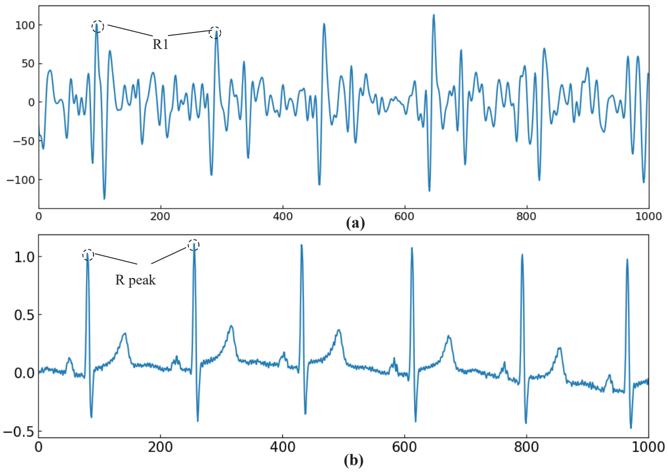

Fig. 2. Thoracic acceleration signal and the corresponding ECG signal

where A is the amplitude of the two baseband signals, θ_0 is the initial phase, and $\Delta\phi$ is the residual phase noise.

Then we use the extended Differentiate and Cross-multiply Algorithm (DACM) to extract the phase information from the I/Q signals to avoid phase fold and improve the noise suppression effect. The phase signal contains respiratory, cardiac activities and other noises. Respiratory movement is usually slow with low acceleration, whereas cardiac activities are rapid contraction of the myocardium, causing significant acceleration during heartbeats [16]. Therefore, we can extract cardiac motions and eliminate respiration by differential filtering based on least square smoothing, which is expressed as:

$$c(t) = \frac{(\phi_{t-3} + \phi_{t+3}) + 2(\phi_{t-2} + \phi_{t+2}) - (\phi_{t-1} + \phi_{t+1}) - 4\phi_t}{16h^2} \tag{3}$$

where h is the frame periodicity between consecutive samples, $c(t)$ is the acceleration information of chest vibration.

The frequency range of respiratory motion and cardiac motion are mainly distributed in the range of 0.1-0.5 Hz and 0.9-2 Hz, respectively. Therefore, a Butterworth Bandpass Filter is used to filter out respiratory and other noise, retaining the chest acceleration signal. Then it is down-sampled to 200 Hz. The Fig. 2(a) and Fig. 2(b) show the acceleration signal and the corresponding ECG signal, respectively. The horizontal axis in the Fig. 2 represents the number of points. After the R peak of the ECG, we observed a distinct $R1$ peak in the acceleration signal, which is consistent with the physiological principle that the mechanical activity of the heart follows the electrical activity [17]. In summary, the acceleration signal can describe the mechanical activity of the heart effectively.

B. Spatiotemporal Model

Modeling cardiac spatiotemporal features with a deep learning network is a significant challenge. To address this, our study integrates the structure of CNN and BiLSTM to map from cardiac motion input to ECG signal output, which is shown in Fig. 1 (d).

The acceleration signal X first passes through a CNN block that contains a one-dimensional convolution layer, an activation layer, and a pooling layer.

$$P = \text{Maxpool}\left(\text{ReLU}\left(\text{Conv1D}(X)\right)\right) \tag{4}$$

Then, the output features P passes through a BiLSTM block, which contain forward and backward LSTM cells to obtain contextual information. This structure enables simultaneous awareness of past and future context for each element in sequence, improving the modeling capabilities of time series data significantly. The output h is expressed as:

$$h = [h_{\text{forward}}, h_{\text{backward}}] \tag{5}$$

As a result, the CNN part extracts the spatial dimension, and the BiLSTM part extracts the temporal dimension of the signal. Therefore, we can accurately reconstruct the ECG signal from the radar signal.

III. EXPERIMENT

A. Dataset

A publicly available dataset provided by Schellenberger et al [18] is used in this study, which comprises simultaneous data collected from a 24GHz radar and a reference device. The data for the experiment contains 30 healthy subjects (14 males and 16 females) during resting scenario. The measurement duration of each person is at least 10 min, and the total duration is about 5 h. The distance between the radar and subjects is around 40 cm. The details are shown in Table I.

B. Implement Details

The experiment is implemented by using PyTorch library [19], select Mean Absolute Error (MAE) loss as the loss function for network training, and use the Adam optimizer to minimize the loss function [20]. The learning rate is 0.001 and the batch size is 16. To ensure model generalization and prevent data leakage, the dataset was split at the patient level into a training set and a test set in a ratio of 80% and 20%, respectively. The input to the network is segmented using a 512-sliding window. The convolutional layer configured with 64 filters and a kernel size of 3. This is followed by a Rectified Linear Unit (ReLU) activation and a Max Pooling layer with both kernel size and stride set to 2. The BiLSTM module comprises 4 layers with a hidden size of 128 units per direction. Moreover, a dropout layer with a dropout rate of 0.2 and an early stopping strategy are introduced to prevent overfitting.

C. Evaluation Metrics

We use the following metrics:

1) Pearson correlation coefficient (PCC): The morphological accuracy of the reconstructed signal.

2) Root mean squared error (RMSE): It is another morphological accuracy, which measures the differences between the reconstructed and ground-truth ECG.

3) Mean absolute error (MAE): NeuroKit2 [21] is used to accurately detect R-peaks and calculate the average absolute

TABLE I. Dataset information

Parameter	Value
Scenarios	Resting
Radar device	24-GHz radar
ECG device	Three channel ECG
Radar raw data	I/Q signals
Radar/ECG frequency	2000 Hz
Total duration	5 h

TABLE II. Results of DST and other models

Models	PCC	MAE(ms)
CNN [14]	0.86	102.2
encoder-decoder [15]	0.91	9
ECGDiff [22]	0.93	-
SS-S2SA [23]	0.92	8.1
DST-s	0.93	6.25
DST-L	0.937	27.5
DST	0.981	5.0

error between the reconstructed and ground-truth ECG. It is the timing precision of the reconstruction results.

In this article, a better reconstruction result should be one in which the deviation between the reconstructed and ground-truth values is as small as possible and the correlation coefficient is as high as possible.

IV. RESULTS AND DISCUSSION

A. Performance Analysis of Different Models

To fully evaluate the model performance of DST, we compare it with several models. Table II presents the results of these models, employing various evaluation metrics.

1) CNN [14]: It uses body surface displacement signal from FMCW radar as the input. The correlation coefficient is 0.86. The MAE of R peak is 102.2 ms.

2) Encoder-decoder [15]: It uses encoder-decoder structure to reconstruct ECG signal from radio frequency (RF) signal. It can be seen that during normal-breath, the PCC and R peak MAE are 0.91 and 9 ms, respectively.

3) ECGDiff [22]: It bases on conditional denoising diffusion models achieves a PCC of 0.93.

4) SS-S2SA [23]: It combines signal segmentation and deep learning (Sequence-to-sequence and attention) to achieve ECG signal reconstruction. The results showed that PCC and R peak MAE are 0.92, 8.1 ms, respectively.

5) DST-s: It is a version of DST without differential filtering algorithm based on least squares smoothing. That is to say, the phase information is used as the input of the model. The result shows that the PCC, RMSE and peak MAE between reconstructed and ground-truth ECG are 0.93, 0.17, 6.25 ms, respectively.

6) DST-L: It is a version of replacing BiLSTM in DST with LSTM, which achieve the PCC, RMSE and peak MAE between reconstructed and ground-truth ECG are 0.937, 0.231, 27.5ms, respectively.

7) DST: The method proposed in this article, which achieve the PCC, RMSE and peak MAE between reconstructed and ground-truth ECG are 0.981, 0.17, 5.0ms, respectively. Using bootstrapping with 1,000 resamples, the 95% CI for the PCC was [0.91, 0.93]. The narrow confidence interval further supports the robustness of this method in the dataset.

Compared with CNN [14], the results of DST indicate that differential filtering based on least squares smoothing and BiLSTM can effectively improve the performance. Compared with [15], there is a significant improvement in PCC, which indicates that proposed method has higher morphological accuracy. Compared with ECGDiff [22], DST showed a 5.5% increase in median PCC. Compared with SS-S2SA [23], the results achieved a 6.6% improvement in median PCC and a 38.3% reduction in median MAE. Compared with DST-s, it can be seen that the differential filter performed on phase information based on least-squares smoothing can effectively reduce the impact of respiration, achieving a 5.5% improvement in PCC and a 20% reduction in MAE. Compared with DST-L, the results indicate that more comprehensive contextual information can be obtained by BiLSTM, achieving a 4.7% improvement in PCC and an 81.8% reduction in MAE. These underscore the robustness of DST method in accurately reconstructing ECG signal.

In summary, the proposed model fused filters for noise reduction, CNN to extract spatial features and BiLSTM to obtain long-term dependencies, addressing the difficulty of balancing temporal and spatial features in previous standard architectures. It demonstrates superior performance across other methods, showcasing its ability to effectively and accurately reconstruct ECG signal from radar signal.

B. Accuracy of Signal Reconstruction

First, we analyze the morphology accuracy. Fig. 3 (a) plots the cumulative distribution functions (CDF) of RMSE. The median RMSE is 0.07 and the 90-percentile RMSE is 0.17, indicating a high level of accuracy. Fig. 3 (b) plots the CDF of PCC. The median PCC is 0.965 and the 90-percentile PCC is 0.981, further affirming the fidelity of the reconstructed signal. Fig. 3 (c) and (d) show two segments of reconstructed ECG and the ground-truth, where the RMSE is 0.047 and 0.059 and PCC is 0.982 and 0.974, respectively. The horizontal axis in the Fig. 3 (c) and (d) represents the number of points. We can see that the reconstructed ECG is basically same with the ground-truth when it has low RMSE and high correlation.

Then, we evaluate the precision of reconstructed ECG timing by detecting R-peaks and calculate the MAE between the reconstructed and ground-truth signal. Fig. 4(a) plots the CDF of MAE. Fig. 4(b) plots the boxplot of MAE. It can be seen that the 90-percentile MAE is 5.0 ms. After removing outliers, the median MAE is only 2.5 ms. It further validates the accuracy of DST in reconstructing ECG signal and its ability to capture cardiac timing, which is crucial for clinical diagnosis and analysis.

C. Discussion and Limitations

The ability to reconstruct ECG signals from mmWave radar with a high morphological fidelity demonstrates a highly consistent, learnable non-linear mapping between the mechanical activity of the heart and its underlying electrical activity. Achieving such precision—particularly in capturing critical morphological features such as the QRS complex and R-R

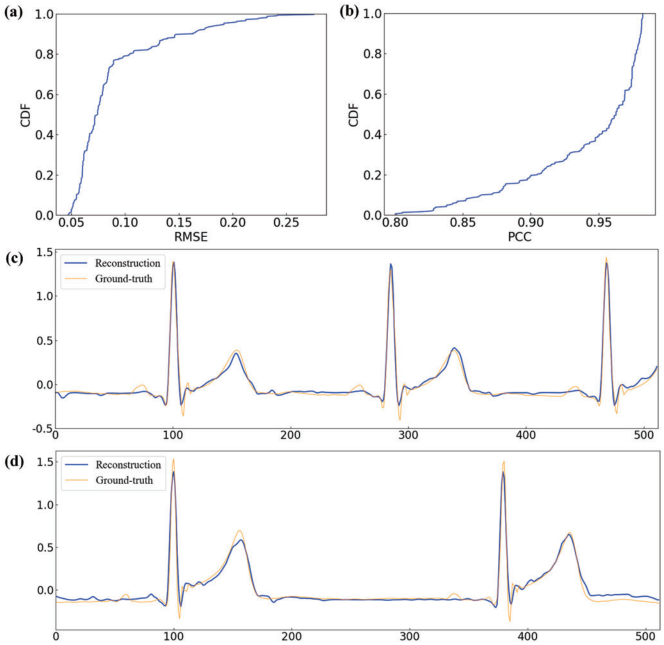

Fig. 3. Morphology accuracy (a) CDFs of RMSE (b) CDFs of PCC (c) and(d) reconstructed and ground-truth ECG

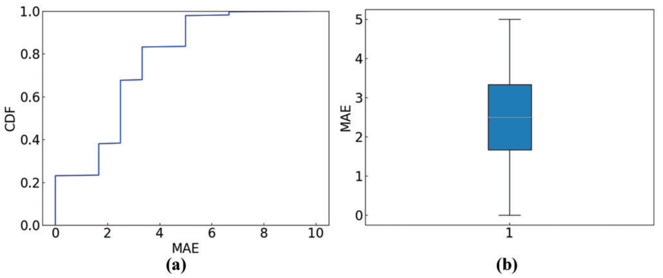

Fig. 4. Precision of reconstructed ECG timing (a) CDF of MAE (b) Boxplot

intervals in a resting scenario—validates the feasibility of utilizing non-contact radar signals as a viable surrogate for traditional contact-based electrodes. Clinically, this method lays a solid foundation for continuous, non-intrusive cardiovascular monitoring. It offers a promising pathway for early screening of arrhythmias and long-term monitoring.

The robust reconstruction performance achieved in our study can be largely attributed to the synergistic architecture of the proposed model. Firstly, the preprocessing module acts as a critical prerequisite, effectively isolating the subtle cardiac vibrations from respiratory and other noise, thereby feeding a purified mechanical signature into the deep learning model. Secondly, the CNN layers are exceptionally suited for extracting spatial features. They effectively capture the sharp phase variations in the radar echo and accurately map them to the sharp morphological peaks of the QRS complex. Finally, the BiLSTM network plays an indispensable role in modeling the long-term temporal dependencies. Together, this hybrid architecture guarantees a reconstructed ECG waveform that is both morphologically accurate and biologically plausible.

There are several limitations of the current study must be acknowledged. First, the experimental setup was constrained to a single, fixed detection distance of 40 cm. Given the non-linear attenuation of radio frequency signals over distance, the current model may experience performance degradation if applied to varying ranges without recalibration. Second, data collection was conducted under resting conditions. In practical, continuous monitoring scenarios, random body movements or postural changes introduce severe motion artifacts that can easily overwhelm the subtle cardiac micro-vibrations.

In the future, we plan to integrate advanced adaptive filtering techniques to combat motion artifacts and expand our dataset through clinical collaborations to incorporate a wider spectrum of physiological and pathological profiles. This will enable the technology to transition from a highly controlled experimental environment to robust real-world applications, ultimately driving the development of a non-contact cardiovascular health monitoring paradigm.

V. CONCLUSION

We proposed DST, an ECG signal reconstruction method that combines the interpretability of signal differential algorithm and complex time series processing capabilities of spatiotemporal learning model. The experimental results on the Nature dataset show that the proposed method can reconstruct the ECG waveform with a smaller error, verifying the accuracy and reliability of the method. The result quantitatively validates the strong electromechanical coupling of the heart and proves the feasibility of extracting precise cardiac electrical signatures from mechanical chest wall micro-displacements. Furthermore, rigorous statistical evaluations confirmed the underlying robustness and reliability of the proposed model. Although the current validations are focused on resting scenarios and fixed distances, the result provides a solid physical and computational foundation for future cardiology analysis. Future efforts will focus on mitigating dynamic motion artifacts and expanding the dataset, ultimately realizing its clinical potential in continuous, non-invasive healthcare settings.

REFERENCES

[1] C. S. Elayi, R. J. Charnigo, P. M. Heron, B. K. Lee, and J. E. Olgin, ‘Primary Prevention of Sudden Cardiac Death Early Post-Myocardial Infarction: Root Cause Analysis for Implantable Cardioverter–Defibrillator Failure and Currently Available Options’, Circ: Arrhythmia and Electrophysiology, vol. 10, no. 6, p. e005194, Jun. 2017.

[2] M. Naghavi et al., ‘From Vulnerable Plaque to Vulnerable Patient—Part III: Executive Summary of the Screening for Heart Attack Prevention and Education (SHAPE) Task Force Report’, The American Journal of Cardiology, vol. 98, no. 2, pp. 2–15, Jul. 2006.

[3] C. E. Hunt, ‘Sudden infant death syndrome’, Canadian Medical Association Journal, vol. 174, no. 13, pp. 1861–1869, Jun. 2006.

[4] J. Diedler, M. Sykora, E. Juttler, T. Steiner, and W. Hacke, ‘Intensive Care Management of Acute Stroke: General Management’, International Journal of Stroke, vol. 4, no. 5, pp. 365–378, Oct. 2009.

[5] R. Guan, S. Yao, X. Zhu, KL. Man, EG. Lim, J. Smith et al., ‘Achelous: A Fast Unified Water-surface Panoptic Perception Framework based on Fusion of Monocular Camera and 4D mmWave Radar’, 2023 IEEE 26th International Conference on Intelligent Transportation Systems (ITSC), Bilbao, Spain, 2023, pp. 182-188.

[6] F. Luo, S. Khan, A. Li, Y. Huang, and K. Wu, ‘EdgeActNet: Edge Intelligence-Enabled Human Activity Recognition Using Radar Point Cloud’, IEEE Trans. on Mobile Comput., vol. 23, no. 5, pp. 5479–5493, May 2024.

[7] J. C. Lin, ‘Noninvasive microwave measurement of respiration’, Proc. IEEE, vol. 63, no. 10, pp. 1530–1530, 1975.

[8] D. Zhang, Y. Hu, and Y. Chen, 'MTrack: Tracking Multiperson Moving Trajectories and Vital Signs with Radio Signals', IEEE Internet Things J., vol. 8, no. 5, pp. 3904–3914, Mar. 2021.
[9] M. Mercuri, I. R. Lorato, Y.-H. Liu, F. Wieringa, C. V. Hoof, and T. Torfs, 'Vital-sign monitoring and spatial tracking of multiple people using a contactless radar-based sensor', Nat Electron, vol. 2, no. 6, pp. 252–262, Jun. 2019.
[10] M. Arsalan, A. Santra, and C. Will, 'Improved Contactless Heartbeat Estimation in FMCW Radar via Kalman Filter Tracking', IEEE Sens. Lett., vol. 4, no. 5, pp. 1–4, May 2020.
[11] N. T. Phuong Nguyen, P.-Y. Lyu, M. H. Lin, C.-C. Chang, and S.-F. Chang, 'A Short-Time Autocorrelation Method for Noncontact Detection of Heart Rate Variability Using CW Doppler Radar', in 2019 IEEE MTT-S International Microwave Biomedical Conference (IMBioC), Nanjing, China: IEEE, May 2019, pp. 1–4.
[12] Z. L. Xia, X. Huai Wang, H. B. Wei, and Y. Xu, 'Detection of Vital Signs Based on Variational Mode Decomposition Using FMCW Radar', in 2021 International Conference on Microwave and Millimeter Wave Technology (ICMMT), Nanjing, China: IEEE, May 2021, pp. 1–3.
[13] U. Ha, S. Assana, and F. Adib, 'Contactless seismocardiography via deep learning radars', in Proceedings of the 26th Annual International Conference on Mobile Computing and Networking, London United Kingdom: ACM, Sep. 2020.
[14] D. Toda, R. Anzai, K. Ichige, R. Saito, and D. Ueki, 'ECG Signal Reconstruction Using FMCW Radar and Convolutional Neural Network', in 2021 20th International Symposium on Communications and Information Technologies (ISCIT), Tottori, Japan: IEEE, Oct. 2021, pp. 176–181.
[15] J. Chen, D. Zhang, Z. Wu, F. Zhou, Q. Sun, and Y. Chen, 'Contactless Electrocardiogram Monitoring with Millimeter Wave Radar', IEEE Trans. on Mobile Comput., vol. 23, no. 1, pp. 270–285, Jan. 2024.
[16] M. Zhao, 'Emotion Recognition using Wireless Signals', Proceedings of the 22nd annual international conference on mobile computing and networking. 2016: 95-108.
[17] O. T. Inan et al., 'Ballistocardiography and Seismocardiography: A Review of Recent Advances', IEEE J. Biomed. Health Inform., vol. 19, no. 4, pp. 1414–1427, Jul. 2015, doi:10.1109/JBHI.2014.2361732.
[18] S. Schellenberger et al., 'A dataset of clinically recorded radar vital signs with synchronised reference sensor signals', Sci Data, vol. 7, no. 1, p. 291, Sep. 2020, doi: 10.1038/s41597-020-00629-5.
[19] A. Paszke, S Gross, F Massa, et al., 'PyTorch: An Imperative Style, High-Performance Deep Learning Library', Advances in neural information pro-cessing systems, 2019, 32.
[20] D. P. Kingma and J. Ba, 'Adam: A Method for Stochastic Optimization', Jan. 30, 2017, arXiv: arXiv:1412.6980. doi: 10.48550/arXiv.1412.6980.
[21] D. Makowski et al., 'NeuroKit2: A Python toolbox for neurophysiological signal processing', Behav Res, vol. 53, no. 4, pp. 1689–1696, Aug. 2021.
[22] K. Feghoul, M. Bouazizi, R. Feghoul, T. Ohtsuki, 'ECGDiff: Conditional Diffu-sion Model for ECG Reconstruction from Doppler Signals', in ICC 2024 - IEEE International Conference on Communications, Denver, CO, USA: IEEE, Jun. 2024, pp. 232–237.
[23] R. Cui, W. Cui, Y. Cai, Y. Yan, 'Non-Contact Reconstruction of ECG signal Using FMCW Radar and SS-S2SA Network', IEICE Trans. Commun., vol. E108-B, no. 2, pp. 208–219, Feb. 2025.